924

Carbon Vol. 27, No. 4, pp. 549–559, 1989
Printed in Great Britain.

0008-6223/89 $3.00 + .00

DETECTION OF LOW TEMPERATURE CARBON GASIFICATION USING DSC AND TGA

I. M. K. ISMAIL† and P. L. WALKER, JR.
Department of Materials Science and Engineering, The Pennsylvania State University, University Park, Pennsylvania 16802, USA

(*Received* 19 *October* 1988; *accepted in revised form* 4 *January* 1989)

Abstract—The interaction of O_2 with Saran char was followed in the temperature range 77–222°C using differential scanning calorimetry and thermal gravimetric analysis. At 77°C oxygen chemisorption was accompanied by O_2 physical adsorption. At 100°C only oxygen chemisorption was detected, making possible the calculation of enthalpy of chemisorption. At 125°C and above oxygen chemisorption was accompanied by char gasification. It was possible, using some reasonable assumptions, to separate these two processes and obtain rates for each. Rates of char gasification were orders of magnitude higher than predicted by extrapolation of high temperature (450–550°C) Zone I gasification data. It suggests that super active sites exist at low temperatures which are rapidly annealed out at higher temperatures and thus do not take part in char gasification.

Key Words—Saran, gasification, TGA, DSC.

1. INTRODUCTION

We previously reported on rates and heats of oxygen chemisorption on Saran chars at 100°C[1] using differential scanning calorimetry (DSC) and thermal gravimetric analysis (TGA). A chemisorption temperature of 100°C was chosen since physical adsorption of O_2 and carbon gasification were negligible at this temperature. We were also interested in obtaining chemisorption results at temperatures somewhat above 100°C (at least up to 250°C), thinking that carbon gasification in 0.1 MPa O_2 would continue to be negligible in this temperature range. Certainly, as will be seen, gasification rates measured at higher temperature, when extrapolated to lower temperatures, would have suggested this to be the case. However, the use of sensitive heat and weight measurements uncovered a "super" reactivity of Saran char at low temperatures.

2. EXPERIMENTAL

2.1 *Materials used*

Saran 498, supplied by Dow Chemical Company, was chosen as the precursor for preparing the carbon used in the study. The sample is a copolymer of vinylidene chloride and vinyl chloride in an approximate mole ratio of 90 to 10. The sample was heated to 900°C and held for 4 h in a flowing dry, high purity N_2 stream. Under these conditions, chlorine is liberated stoichiometrically as HCl, leading to the production of microporous char[2,3]. Neutron activation analysis found <6 ppm chlorine remaining in the char.

The char was ground in a quartz lab mortar. The 57 × 100 μm fraction was used. The sample (called S_4) was analyzed for metal impurities (possible catalysts) using emission spectroscopy. The following elements in ppm, on a weight basis, were detected: Fe, 20; B, <10; Al, 10; Ca, 5; Si, 50; and Cu, 3. The following elements, in ppm, were not detected. If present, they are below the levels given: Mg, 2; Be, 1; Sr, 2; Ba, 10; Mn, 10; V, 10; Ti, 2; Co, 10; Pb, 20; Zr, 5; Ni, 10; Ag, 1; Nb, 10; Cr, 10; Mo, 5; Zn, 50; Bi, 10; and Sn, 10.

Part of the S_4 sample (called S_{act}) was activated in a fluidized bed by exposure to air at 425°C for 10 h. Weight loss due to gasification was 63.8%.

Surface areas, measured by N_2 uptake at 77K (BET) and CO_2 uptake at 298K (Polanyi–Dubinin), were 808 and 1140 m^2/g and 1156 and 1210 m^2/g for the S_4 and S_{act} samples, respectively.

Ultrahigh-purity N_2 had a minimum purity of 99.9999% with a moisture content of <1 ppm. Dry-grade O_2 had a minimum purity of 99.997% and a moisture content of <3 ppm.

2.2 *DSC and TGA apparatus*

A Dupont DSC cell was used in conjunction with a cell base Module-II and a 990 Thermal Analyzer. This apparatus and its calibration are completely described elsewhere[1,4].

A TGA apparatus was constructed to match the performance and accuracy obtained with the DSC apparatus. The major components of the TGA apparatus were a Cahn RG weighing mechanism placed in a glass vacuum bottle electrobalance, which in turn was connected to a vertical Vycor tube. The TGA apparatus is completely described elsewhere[4].

†Air Force Rocket Propulsion Laboratory, AFRPL/MKBN Mail Stop #24, Edwards Air Force Base, California 93523-5000, USA.

2.3 *Operating procedure*

The operating procedure used with both apparatuses was basically the same. In the case of DSC, a known weight of sample (usually 10–12 mg) was placed on the quartz sample pan. The pan was placed in the sample platform inside the cell. In the case of the TGA, a sample weight (between 50 and 100 mg) was placed in a quartz bucket and then suspended inside the reactor. The DSC cell or TGA reactor was outgassed down to 0.13 kPa for 15 min and then flushed with 0.1 MPa N_2 flowing at 45 cm^3/min. The sample was heated at 20°C/min from ambient temperature to 600°C, held at this temperature for 30 min, and then cooled to room temperature. Thereafter, the sample was heated isothermally for 30 min in 0.1 MPa N_2 at a chosen reaction temperature. At the end of this period, 0.1 MPa O_2 was introduced over the sample to replace N_2, at the same flow rate. With the DSC apparatus, the scan was started, and the output thermogram was recorded for a 28-min reaction time. With the TGA apparatus, weight changes were monitored as a function of time for a period of 0.5–48 h, depending on the information desired. The sensitivity of weighing was such that meaningful data could be obtained over much longer times in the TGA apparatus than was the case in the DSC apparatus.

2.4 *Measurement of active surface area*

Since it was not possible to produce a good vacuum in the DSC apparatus and further since the maximum temperature attainable was 700°C, it was clear that chemisorption measurements in the apparatus would be carried out on chars which already had a significant fraction (θ) of their active surface covered with oxygen. It has previously been shown[5,6] that, essentially, a carbon surface "cleaned" of oxygen complex can be produced by heating to 950°C in an ultrahigh vacuum. That is, at this temperature "all" oxygen complex is unstable, coming off as CO and CO_2. Thus, as previously described[5,6], a volumetric adsorption apparatus attached to a mass spectrometer was used to determine the total active surface areas (ASA). A char sample was evacuated at room temperature down to a pressure of 0.1 μPa, followed by heating at 20°C/min to 950°C and holding until the pressure dipped to 10 μPa and remained constant for 24 h. The sample was then cooled under vacuum to 100°C, and 0.1 MPa O_2 was introduced. A hold time of 48 h proved more than sufficient for detectable oxygen chemisorption to be completed. Following this hold time, the system was evacuated to 0.1 μPa and the temperature then raised to 950°C to desorb chemisorbed oxygen as CO and CO_2, as previously described[5,6]. For calculating ASA, a value of 0.083 nm^2 was assigned to the average area occupied by one oxygen atom chemisorbed on one carbon site on the prismatic planes of the surface[7]. The ASA's of samples S_4 and S_{act} were 37 and 52 m^2/g, respectively, that is 3.2 and 4.3% of the total surface area as measured by CO_2 adsorption.

As stated previously, prior to a chemisorption run the sample was heated to 600°C in 0.1 MPa N_2 and held at this temperature for 30 min. It was of interest to estimate what the surface coverage (θ) with oxygen was following this pretreatment. To estimate this, a sample, following pretreatment, was exposed to 0.1 MPa O_2 at 100°C for 48 h in the TGA apparatus. This was more than ample time for oxygen chemisorption to be completed. If the weight of this oxygen pick up is designated as W_{tot} and total oxygen pickup following outgassing at 950°C is designated as W_{ASA}, θ at the start of chemisorption runs in the DSC and TGA apparatus is given by

$$\theta = \frac{W_{ASA} - W_{tot}}{W_{ASA}} \quad (1)$$

Fractional surface coverage prior to the start of runs is estimated as 0.68.

3. RESULTS AND DISCUSSION

3.1 *Physical adsorption of O_2*

Processes which may accompany oxygen chemisorption on carbon are physical adsorption of O_2 and carbon gasification. The presence of physical adsorption was detected in the usual way. A first adsorption run was made in the TGA apparatus by exposure to 0.1 MPa O_2 until no further weight increase was observed. The sample was then outgassed at adsorption temperature to remove physically adsorbed O_2, followed by the reintroduction of 0.1 MPa O_2. Under these conditions, an increase in sample weight in the second run was ascribed to the physical adsorption of O_2. At 75°C, physical adsorption could be detected, with equilibrium reached in 15 min. Oxygen uptake was 0.114 mgO_2/g of S_{act} sample, for example. Assuming an area for the O_2 molecule of 0.27 nm^2, this amounts to a fractional monolayer coverage of 4.6×10^{-4}, based on the CO_2 surface area of the S_{act} sample. At 100°C and above, no physical adsorption of O_2 could be detected. This process would thus make no contribution to the heat generated upon exposure of the Saran chars to O_2 at 100°C and above. In fact, even at 75°C heat produced due to physical adsorption of O_2 made only a small contribution to overall heat generated. This is a result of the heat of physical adsorption of O_2 on carbon (4–6 kcal/gmole) being small[8] compared to values for heats of oxygen chemisorption.

3.2 *High temperature gasification rates for Saran chars*

Burn-off plots, as measured by TGA, are shown in Fig. 1 for the reaction between the S_4 sample and 0.1 mPa O_2 between 475 and 550°C. At these temperatures after small amounts of initial carbon burn-off, rates of carbon gasification are dominant over rates of oxygen complex buildup. Hence, weight changes per unit time essentially reflect weight of carbon gasified per unit time. Rates are shown to

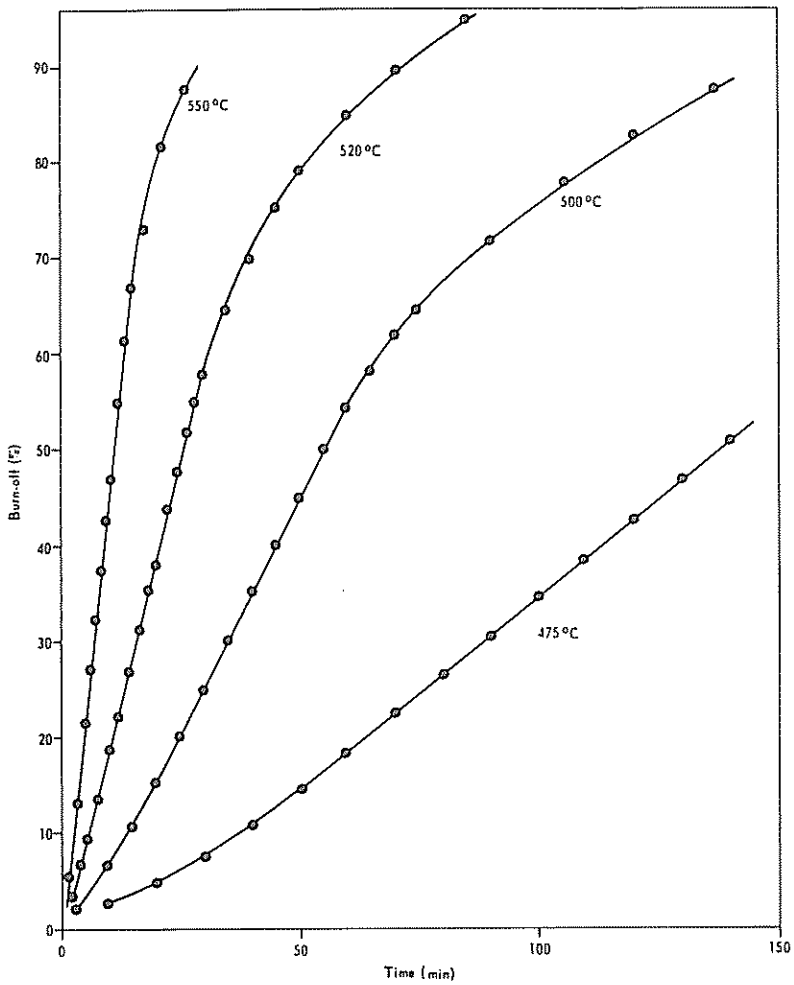

Fig. 1. Gasification of S_1 char in 0.1 MPa O_2 between 475–550°C.

be constant over extended regions of carbon burn-off. These rates are shown on an Arrhenius plot, Fig. 2, along with rates measured at higher gasification temperatures. A familiar Arrhenius plot is seen for carbon gasification, gasification breaking down into Zones I, II, and III[9]. In the low temperature regime (Zone I), the rate is controlled by the inherent chemical reactivity of the Saran char. An activation energy of 42.6 kcal/gmole is typical of that found for carbon gasification in O_2 in Zone I[9]. Extrapolation of the Arrhenius plot in Fig. 2 to temperatures where chemisorption studies will be made yields estimated gasification rates listed in Table 1. These rates are so low that it would be impossible to measure by DSC the heat produced as a result of char gasification by O_2, producing CO_2 in the temperature range 125–227°C. A negligible effect of carbon gasification on TGA measurements would also be expected, based on previous studies[4]. For example, for chemisorption studies at 100°C, the initial rate of measured weight increase due to oxygen chemisorption was ~0.2 mg/gC/min[4].

Further studies were made, in this laboratory, on gasification rates of Saran char in 0.1 MPa air at 375°C, by measuring the rates of CO and CO_2 production[10]. Burn-off was linear with time up to ~50% burn-off, with a rate of 1.9×10^{-1} mg/gC/min. Extrapolation of this rate to 227°C, using an activation energy of 42.6 kcal/gmole, yields an estimated rate of 1.1×10^{-5} mg/gC/min. While higher than the rate predicted previously (Table 1), its effect on chemisorption measurements would also be negligible.

Table 1. Estimated gasification rates of Saran Char in 0.1 MPA O_2 at very low temperatures by extrapolation of high temperature data

Temperature, °C	Rate, mg/gC/min
125	4.2×10^{-11}
150	1.0×10^{-9}
177	2.2×10^{-8}
202	2.7×10^{-7}
227	2.6×10^{-6}

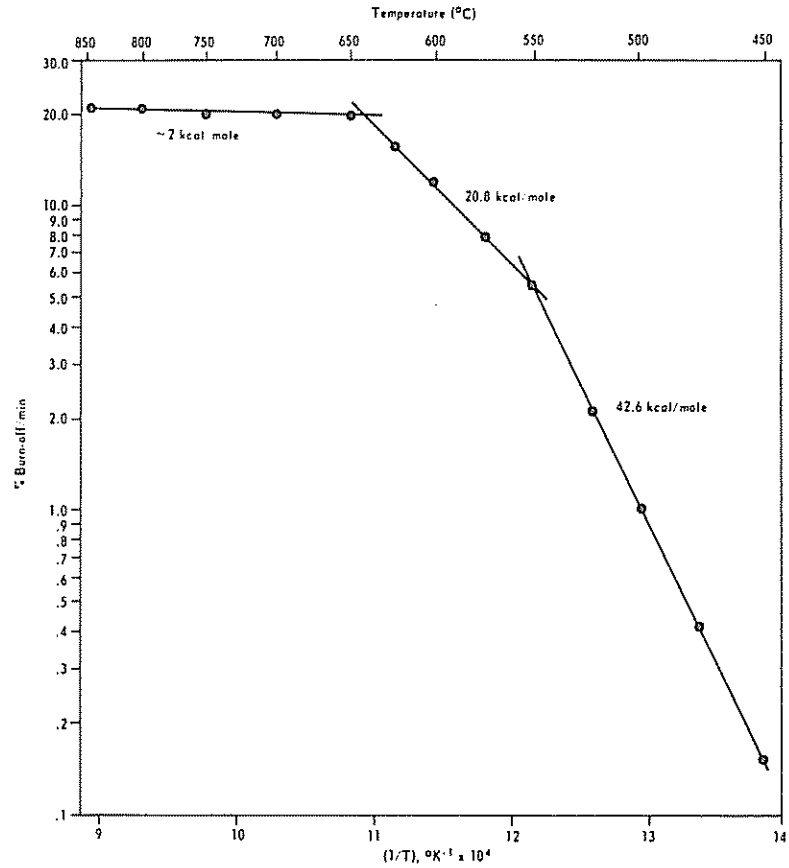

Fig. 2. Arrhenius plot for gasification of S_1 char in 0.1 MPa O_2 between 450–850°C.

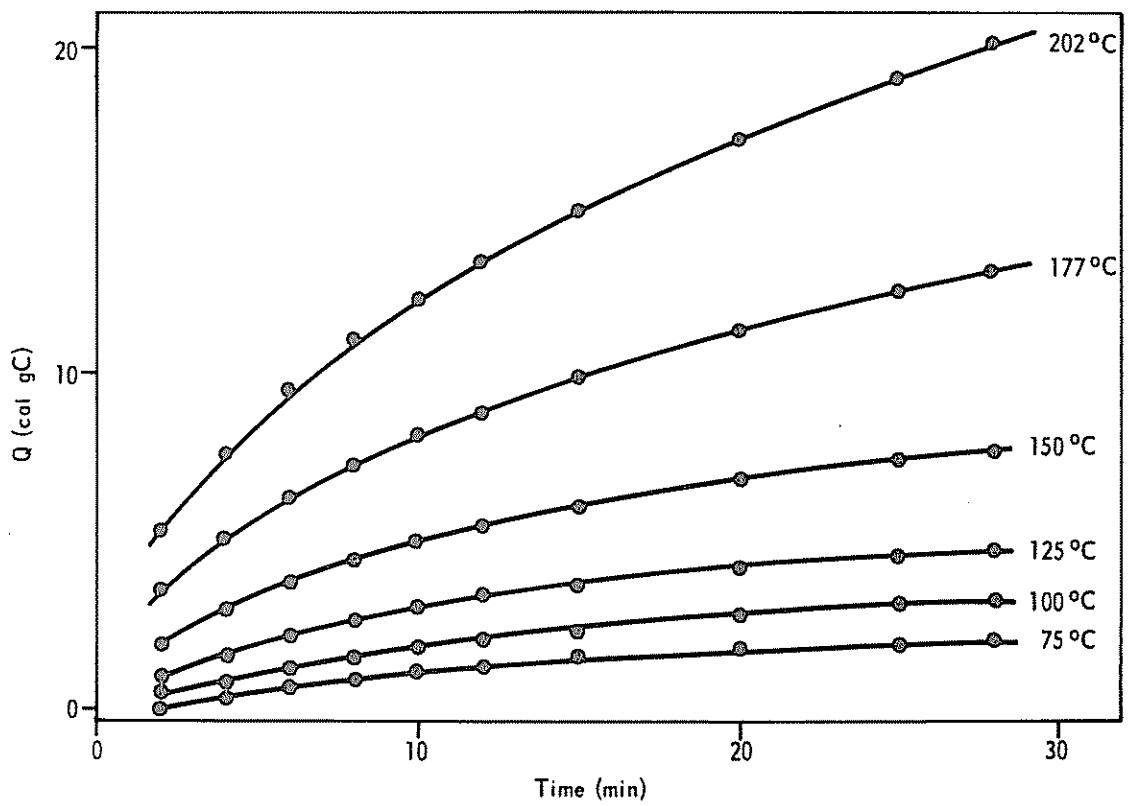

Fig. 3. Heat released during interaction between 0.1 MPa O_2 and S_{act} char between 75–202°C.

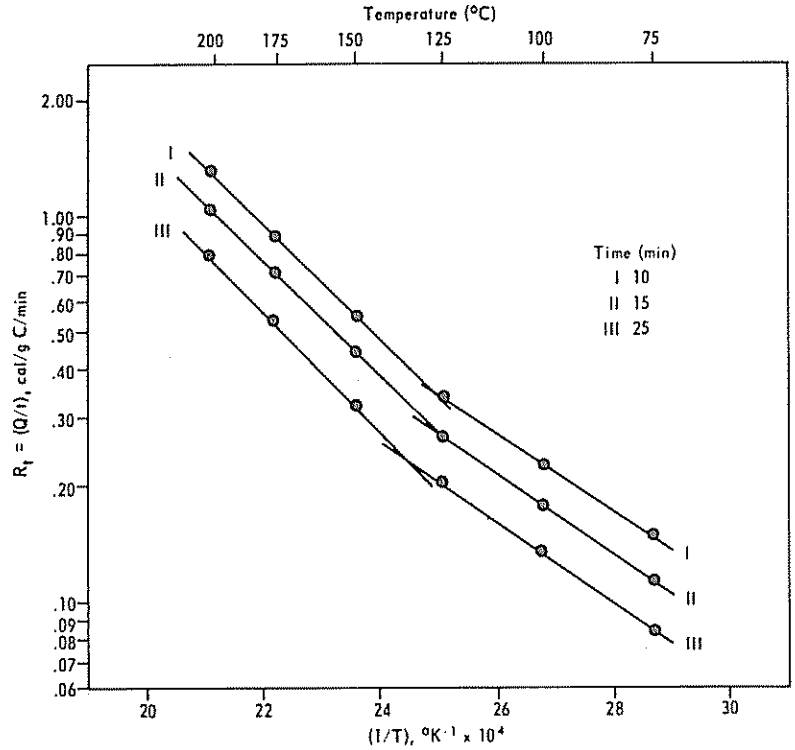

Fig. 4. Arrhenius plots for average heat release rates during interaction between 0.1 MPa O_2 and S_{act} char between 75–202°C at fixed reaction times.

3.3 *Measurements of O_2 interaction with Saran chars between 75–227°C*

3.3.1 *Experimental weight and heat measurements.* Figure 3 presents results for cumulative heat release (Q) as a function of temperature and time for the S_{act} sample upon exposure to 0.1 MPa O_2. At fixed times, Q and rates of heat released (R_t) increase with increasing temperature. At three chosen time intervals, R_t (where $R_t = Q/t$ for t = 10, 15, and 25 min) was calculated for each reaction temperature. Arrhenius plots of R_t are shown in Figure 4 for the S_{act} sample. For each R_t, two linearities are observed, the first linear region starting at 75°C and ending at ~125°C. The second linear region starts at ~125°C and extends at least to 202°C. The calculated activation energies for the first and second regions were 4.7 and 7.2 kcal/gmole, respectively. The values were independent of the reaction time over which the rates were computed. It suggests that for the S_{act} sample the kinetics of the carbon–O_2 interaction below 125°C is different from that above this temperature.

For the S_4 sample, a similar behavior was observed; that is, Arrhenius plots were again discontinuous. The calculated activation energies for the first and second regions were 5.7 and 9.7 kcal/gmole, respectively.

Figure 5 presents results for cumulative weight gain (W_{exp}) as a function of temperature and time for the S_{act} sample upon exposure to 0.1 MPa O_2. Between 75 and 177°C, W_{exp} increases with increasing temperature for fixed values of time. However, for the run at 202°C, W_{exp} is lower than that found at 177°C for fixed values of time. This finding suggests that the weight gain recorded by the TGA at 202°C could, in fact, be the result of two simultaneous reactions taking place at the carbon surface. Oxygen chemisorption is responsible for a weight gain (W_+); carbon gasification is responsible for a weight loss (W_-). Therefore, W_{exp} is given by

$$W_{exp} = W_+ - W_- \qquad (2)$$

Since the activation energy for carbon gasification (W_-) is expected to be higher than the activation energy for the oxygen chemisorption (W_+), it is expected that the importance of carbon gasification to the overall interaction of O_2 with char will increase with increasing reaction temperature and increasing reaction time at fixed temperature[6,9].

Enthalpies of reaction in kcal/gmole O_2, initially assuming that $W_- << W_+$, were calculated from $\Delta H = -32\ Q/W$. They are listed in Table 2 for temperatures of 100 and 125°C. Enthalpies of reaction for the S_{act} sample are essentially independent of reaction time and temperature over the θ range 0.68–0.78. As discussed previously[1] it is concluded from the constancy of ΔH as a function of time and temperature that char gasification for the S_{act} sample at 100–125°C is negligible. For the S_4 sample, ΔH at 100°C is also independent of time and temperature of reaction. The enthalpy of interaction is significantly lower (41 kcal/gmole) for the S_4 sample than that for the S_{act} sample (77 kcal/gmole). It was sug-

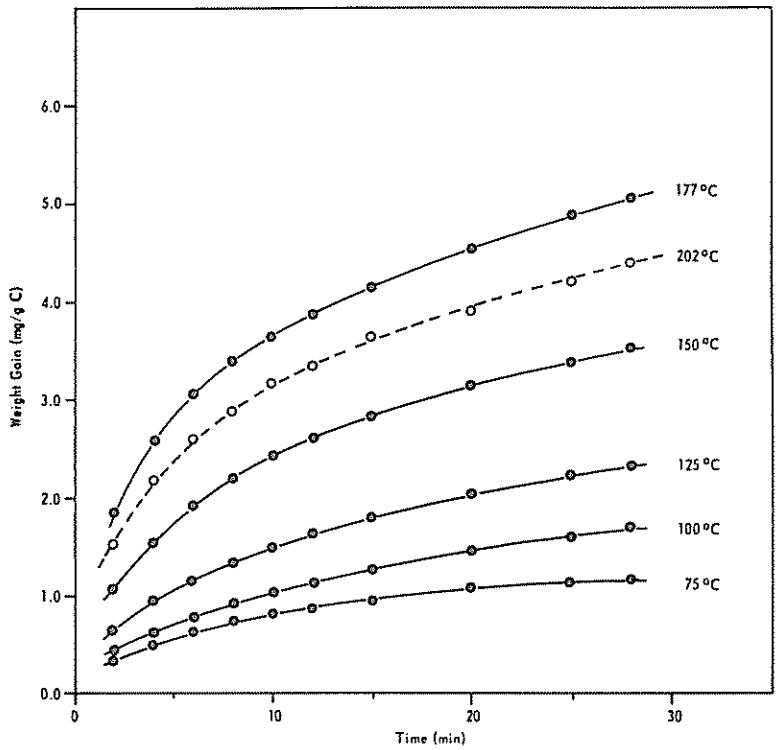

Fig. 5. Weight gained during interaction between 0.1 MPa and S_{act} char between 75–202°C.

gested that this is a result of differences in the make-up of edge terminating carbon sites in these two samples[1]. This in turn would result in differences in the structure of oxygen complexes formed upon chemisorption—differing extents to which lactone and carbonyl groups are formed, for example. For the S_4 sample, reaction at 125°C results in a monotonic increase in $-\Delta H$ with reaction time. As discussed previously[11], apriori or induced heterogeneity would produce a decrease in $-\Delta H$ with increasing time of chemisorption or increasing θ. However, no explanation can be found for increasing $-\Delta H$ with increasing reaction time, if only oxygen chemisorption were occurring. It was, therefore, concluded that oxygen interaction with the S_4 sample at 125°C resulted in two concurrent reactions—oxygen chemisorption and carbon gasification. As reaction time increases, carbon gasification (with a higher value of $-\Delta H$) becomes increasingly more important.

Table 2. Enthalpies of oxygen interaction with Chars

	$-\Delta H$, kcal/gmole O_2			
	100°C		125°C	
Reaction Time, min	S_{act}	S_4	S_{act}	S_4
2	79	42	75	43
10	77	41	76	50
20	77	41	76	54
25	76	42	76	56

At temperatures above 125°C, both samples show apparent increases in $-\Delta H$ with increasing reaction times up to 25 min. For example, for the S_4 sample, the spread in $-\Delta H$ values increases with temperature from 43–56 kcal/gmole at 125°C to 107–164 kcal/gmole at 227°C.

3.3.2 *Separation of oxygen chemisorption from carbon gasification.* When both carbon gasification and oxygen chemisorption are occurring simultaneously, the value of Q measured experimentally, Q_{exp}, involves two terms. Thus

$$Q_{exp} = Q_c + Q_g \tag{3}$$

where Q_c and Q_g are the exothermic heats evolved due to chemisorption and gasification, respectively. If ΔH for oxygen chemisorption can be assumed to be independent of chemisorption temperature, Q_c for the S_4 char is given by

$$Q_c = \left(\frac{41}{32}\right) W_- \tag{4}$$

where W_- and Q_c are expressed in units of mg oxygen/gC and cal/gC, respectively. Or

$$Q_c = 1.281\,(W_{exp} + W_-). \tag{5}$$

When carbon is gasified, the gaseous products are CO and CO_2. The enthalpies of combustion of β–graphite are -27 kcal/gmole and -94 kcal/gmole for the formation of CO and CO_2, respectively. As-

suming that heats of combustion do not vary much with carbon structure and since the atomic weight of carbon is 12, one may introduce

$$Q_g = \left(\frac{27}{12}\right) W_- \tag{6}$$

for the formation of CO and,

$$Q_g = \left(\frac{94}{12}\right) W_- \tag{7}$$

for the formation of CO_2.

When carbon is gasified in O_2, the ratio of CO to CO_2 produced, as a function of temperature, is given by,

$$\frac{CO}{CO_2} = A \exp\left(\frac{-E}{RT}\right) \tag{8}$$

where $E = 6.4$ kcal/gmole, T is the absolute temperature of reaction and R is the gas constant[12]. Values of A range between 100 and 300 depending upon the ASA of the carbon and the fraction of active sites (θ) covered by oxygen complex. In this study A is assumed to equal 150. Following this approach CO/CO_2 ratios can be calculated as a function of temperature and, in turn, enthalpies of combustion per mole of carbon gasified can be calculated. For example, at 227°C

$$Q_g = \left(\frac{82.9}{12}\right) W_- \tag{9}$$

Substituting equations (5) and (9) into equation (3), the weight of S_4 char gasified at 227°C is

$$W_- = 0.122\,(Q_{exp} - 1.281\,W_{exp}) \tag{10}$$

3.3.3 *Experimental low temperature carbon gasi-*

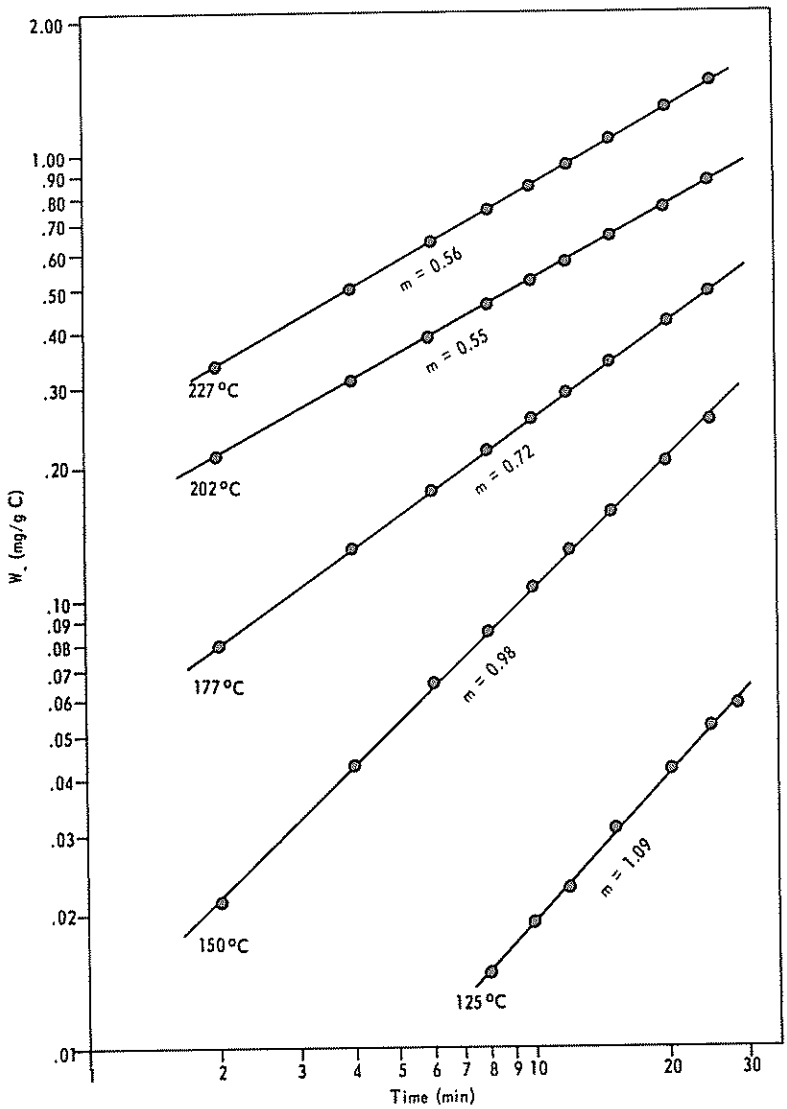

Fig. 6. Estimated weight of S_4 char gasified in 0.1 MPa O_2 as a function of time and temperatures between 125–227°C.

Table 3. Estimated gasification rates of Saran Char in 0.1 MPA O_2 at very low temperatures

Temperature, °C	Rate, mg/gC/min × 10^2	
	10 min	20 min
150	1.1	0.77
177	1.8	1.4
202	3.1	2.0
227	5.0	3.7

fication rates. Figure 6 presents results for W_- vs t on a log-log scale for the S_4 sample at different reaction temperatures. A relationship

$$W_- = B(t)^n \tag{11}$$

is found where both B and n are temperature dependent. Estimated gasification rates (dW_-/dt) for the S_4 samples at temperatures between 150 and 227°C are given in Table 3 at reaction times of 10 and 20 min. These gasification rates between 150 and 227°C are orders of magnitude higher than those predicted by extrapolation of gasification rates measured at higher temperatures (Table 1). However, it is important to emphasize that these gasification rates are still not high. To put them in perspective, it would take 176 min to remove one monolayer of carbon atoms from the ASA of the S_4 char at 227°C.

Rates at 10 min, shown on the Arrhenius plot in Fig. 7, yield an activation energy of ~8 kcal/gmole for char gasification. This activation energy is much lower than that found for gasification of the S_4 char in Zone I at higher temperatures (42.6 kcal/gmole).

Knowledge of both W_+ and W_- as a function of time and temperature also permits calculation of differential gasification rates at constant values of θ. Figure 8 presents results on an Arrhenius plot for $\theta = 0.88$ over the temperature range 177 to 227°C. The data yield an activation energy of ~15 kcal/gmole. This is perhaps the best way to examine carbon gasification results (when appropriate data are available) since gasification will result from a combination of two processes. One process will be direct impingement of O_2 onto vacant carbon active sites, leading to some immediate carbon gasification. The second process will involve surface diffusion of oxygen complex from carbon sites where gasification is not possible to uncovered carbon sites where gasification is possible. The rate of the first process will be proportional to $(1-\theta)^2$. The rate of the second process will be proportional to θ.

There is some uncertainty as to what value to assign to the pre-exponential term A in equation (8) in order to calculate the CO/CO_2 ratios. Minimum values of W_- would be calculated if it was assumed that char gasification led only to CO_2 formation. At 227°C rates of gasification would be 90.2% of those given in Table 3; at 150°C they would be 99.0%. Rates of gasification of chars between 150–227°C are orders of magnitude higher than those predicted from high temperature data regardless of what values are assumed for the CO/CO_2 ratio.

The combination of much higher experimental gasification rates than predicted from higher temperature data and the unusually low activation energies for carbon gasification suggests that reaction at low temperatures is occurring at super active sites. Those super active sites are created by gasification

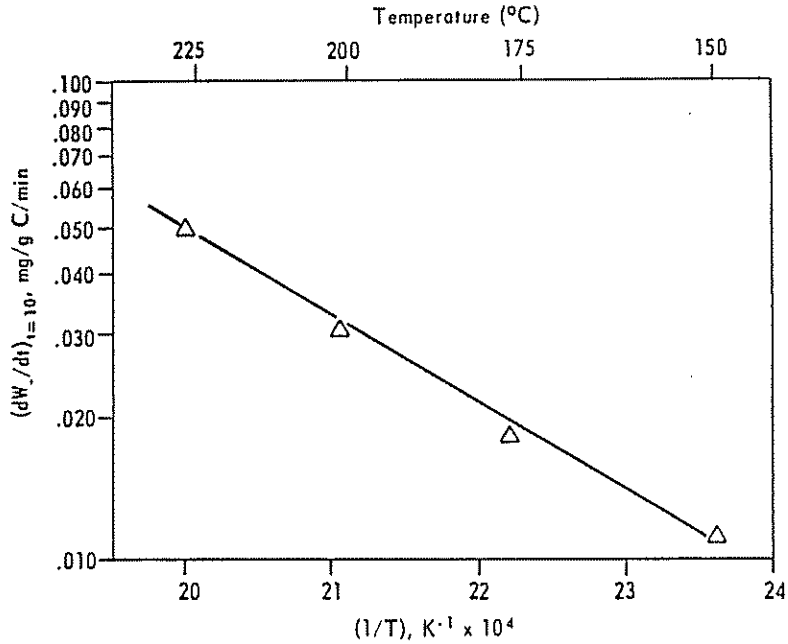

Fig. 7. Arrhenius plot of estimated gasification rates of S_4 char in 0.1 MPa O_2 at 10 min reaction time and temperatures between 150–227°C.

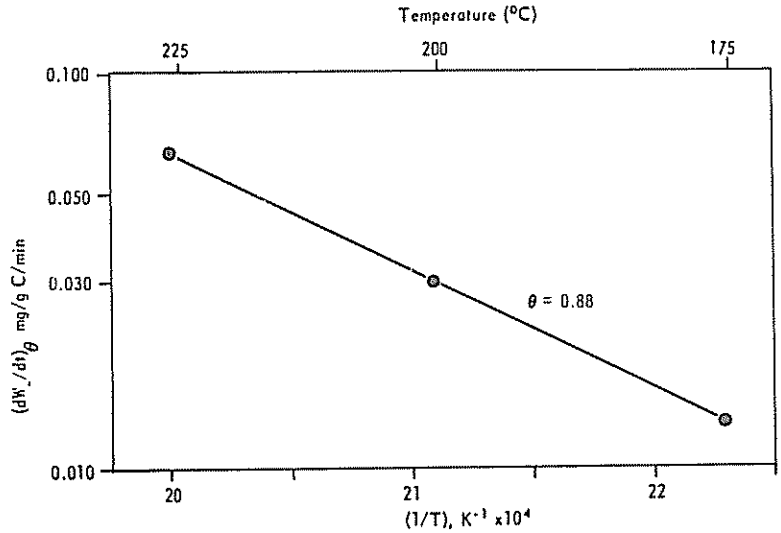

Fig. 8. Arrhenius plot of estimated gasification rates of S_4 char in 0.1 MPa O_2 at constant complex coverage (0.88) and temperatures between 175–227°C.

events and to some extent are preserved (not annealed out to less active sites) prior to the next collision of O_2 with them. As temperature is increased, at some point annealing becomes sufficiently rapid that their removal essentially becomes complete between collision events of O_2 with these sites. It is tempting to suggest that these super active sites are dangling carbon atoms (that is, those not in the condensed arm-chair or zig-zag structures) situated at strategic locations on the prismatic faces in the surface.

3.3.4 *Experimental low temperature oxygen chemisorption rates.* Differential rates of oxygen chemisorption (dW_-/dt) were determined as a function of temperature at constant values of θ. Results are shown on an Arrhenius plot, Fig. 9, for the S_4 sample. Values of activation energy were essentially independent of θ over the coverage range 0.76–0.97, averaging 11.4 ± 0.7 kcal/gmole. Previously, we have suggested that oxygen chemisorption on carbon occurs on different discrete types of sites[6]. The activation energy for chemisorption on one type of site changes little with coverage, but there is an abrupt change in activation energy when chemisorption proceeds from one type of site to another[6]. We previously found for oxygen chemisorption on activated Graphon that there were five distinct regions of chemisorption with the activation energy for chemisorption increasing from 3.1 kcal/gmole at very low coverages in region I to 12.4 kcal/gmole at high cov-

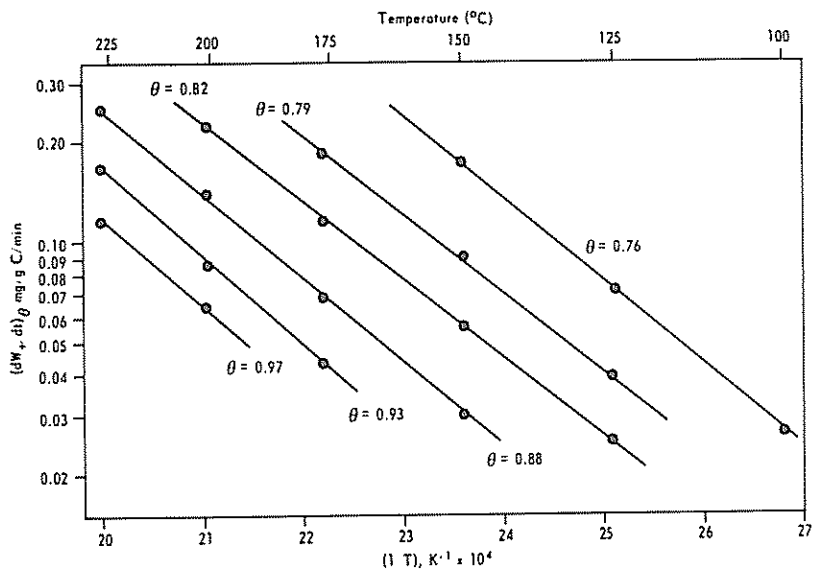

Fig. 9. Arrhenius plots of estimated oxygen chemisorption rates of S_4 char in 0.1 MPa O_2 at different levels of complex coverages and temperatures between 100–227°C.

erages in region V. It is suggested that chemisorption of oxygen on the S_4 sample, considered above, occurred on similar carbon sites on a surface already well covered by oxygen complexes. That chemisorption was occurring on similar carbon sites (forming oxygen complex of similar structure) is also supported by the constancy of ΔH for chemisorption on the S_4 sample as a function of time at 100°C (Table 2).

For the S_4 samples, both W_- and W_- increased over the duration of the runs conducted. It was interesting to follow their increase with time or θ. Figure 10 presents results for the ratio $0.75\ dW_-/dW_-$ as a function of θ. This ratio would also be equal to the ratio $d(O)/d(C)$, or the ratio of change in atoms of oxygen added due to chemisorption to the atoms of carbon lost due to gasification. The relationship is essentially independent of reaction temperature between 125 and 227°C. The ratio decreases rapidly with increasing θ up to ~0.85 and then levels off at a value of 2.0. At short reaction times (or lower values of θ) oxygen chemisorption is predominant. At values of θ close to 1.0, two atoms of oxygen are added for each atom of carbon gasified. Since the primary gaseous species produced at these low temperatures is CO_2, it means that roughly half of the oxygen is being chemisorbed and half is going into the gaseous product, CO_2.

It is to be emphasized that θ values given in Fig. 10 and elsewhere in this paper are based on the equilibrium amount of oxygen chemisorbed at 100°C (in the absence of carbon gasification) as discussed previously. Clearly, in the presence of carbon gasification oxygen complex formation can exceed that found at equilibrium in the absence of carbon gasification. This is seen in Fig. 10 for the longer reaction times at 227°C. Also as θ closely approaches 1.0, $d(O)/d(C)$ should approach zero, which is not found to be the case. It points up the difficulty of using oxygen chemisorption to equilibrium in the absence of gasification to yield a value for ASA in the presence of carbon gasification. The problem was demonstrated previously by Taylor who studied the reactivity of Saran char in the presence of 0.1 MPa air at 375°C[10]. At char burn-offs up to 89.1%, stable oxygen complex formation far exceeded that which was produced, at equivalent burn-offs, during equilibrium oxygen chemisorption in the absence of carbon gasification at 100°C.

As discussed previously, when considering the "inert" gas effect on carbon gasification rates in CO_2[13], it is suggested that a gasification event produces immediately a surface carbon active site possessing an unpaired σ-electron. At some rate, a π-electron will jump from the π-band into the σ-state to form an in-plane σ pair[14]. This leads to a decrease in reactivity of the site to incoming gases. However, if a collision event occurs prior to formation of a σ-pair, the probability of reaction between the incoming gas and the site leading to further carbon gasification or oxygen chemisorption is greater. Thus, in the presence of gasification, the amount of oxygen complex formed can exceed that formed, at equilibrium, in the absence of gasification. Differences will depend upon the O_2 pressure and temperatures used. The lower the O_2 pressure

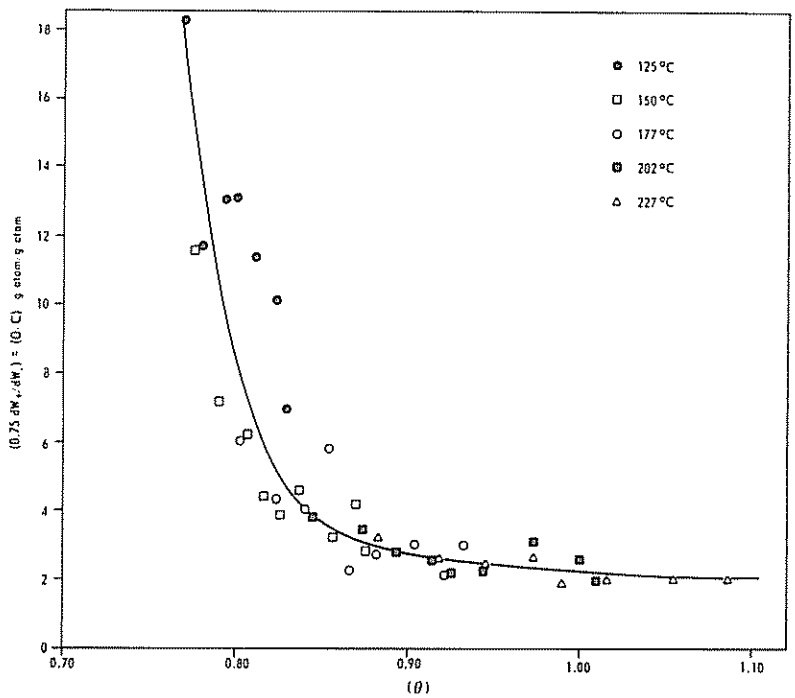

Fig. 10. Dependence of $d(O)/d(C)$ on complex coverage for the S_4 char in 0.1 MPa O_2 at temperatures between 125–227°C.

(or the longer the time between collision events) and the higher the temperature the less effect gasification should have on enhancing oxygen chemisorption. This is borne out by the studies of Laine, *et al.*[7]. Working at a higher temperature (625°C) and a lower O_2 pressure (5 Pa), stable oxygen complex formation during gasification did not exceed that formed at equilibrium in the absence of gasification.

Acknowledgements—This research was made possible by the financial support of the U.S. Department of Energy under Contract EX-76-C-01-2030. Dow Chemical Company kindly supplied the Saran, and Airco Speer Carbon Company kindly carbonized the Saran. Helpful discussions with Dr. O. P. Mahajan are appreciated.

REFERENCES

1. I. M. K. Ismail and P. L. Walker, Jr., *J. Colloid Interface Sci.* **75**, 299 (1980).
2. T. G. Lamond, J. E. Metcalfe III, and P. L. Walker, Jr., *Carbon* **3**, 59 (1965).
3. F. H. Winslow, W. O. Baker, and W. A. Yager, In Proc. 1st and 2nd Conf. Carbon, p. 93. University of Buffalo, Buffalo, New York (1956).
4. I. M. K. Ismail, Ph.D. Thesis, The Pennsylvania State University, 1978.
5. P. L. Walker, Jr., R. C. Bansal, and F. J. Vastola, In The Structure and Chemistry of Solid Surfaces (G. Somarjai, Ed.), pp. 81-1 to 81-16. Wiley, New York (1969).
6. R. C. Bansal, F. J. Vastola, and P. L. Walker, Jr., *J. Colloid Interface Sci.* **32**, 187 (1970).
7. N. R. Laine, F. J. Vastola, and P. L. Walker, Jr., *J. Phys. Chem.* **67**, 2030 (1963).
8. R. L. Gale and R. A. Beebe, *J. Phys. Chem.* **78**, 555 (1964).
9. P. L. Walker, Jr., F. Rusinko, Jr., and L. G. Austin, In Advances in Catalysis, Vol. 11 (D. D. Eley, P. W. Selwood, and P. B. Weisz, Eds.), pp. 133–221. Academic Press, New York (1959).
10. R. L. Taylor, Ph.D. Thesis, The Pennsylvania State University, 1982.
11. M. Boudart, *J. Am. Chem. Soc.* **74**, 3556 (1952).
12. R. Phillips, F. J. Vastola, and P. L. Walker, Jr., *Carbon* **8**, 205 (1970).
13. P. L. Walker, Jr., L. Pentz, D. L. Biederman, and F. J. Vastola, *Carbon* **15**, 165 (1977).
14. H. T. Pinnick, In Proc. 1st and 2nd Conf. Carbon, p. 3. University of Buffalo, Buffalo, New York (1956).